Marine Pollution Bulletin 74 (2013) 344–350

Contents lists available at SciVerse ScienceDirect

Marine Pollution Bulletin

journal homepage: www.elsevier.com/locate/marpolbul

Distribution of local ^{137}Cs anomalies on the seafloor near the Fukushima Dai-ichi Nuclear Power Plant

Blair Thornton [a,*], Seiki Ohnishi [b], Tamaki Ura [a,1], Naoteru Odano [b], Shun Sasaki [a], Tsuneo Fujita [c], Tomowo Watanabe [d], Kaoru Nakata [e], Tsuneo Ono [d], Daisuke Ambe [d]

[a] Institute of Industrial Science, The University of Tokyo, 4-6-1 Komaba, Meguro-ku, Tokyo 153-8505, Japan
[b] National Maritime Research Institute, 6-38-1 Shinkawa, Mitaka-shi, Tokyo 181-0004, Japan
[c] Fukushima Prefectural Fisheries Experimental Station, 13-2 Aza-Matsushita, Shimokajiro, Onahama, Iwaki-shi, Fukushima 970-0316, Japan
[d] National Research Institute of Fishery Science, Fisheries Research Agency, 2-12-4 Fukuura, Kanazawa, Yokohama, Kanagawa 236-8648, Japan
[e] Fisheries Research Agency, 15F Queen's Tower B, 2-3-3 Minatomirai, Nishi-ku, Yokohama, Kanagawa 220-6115, Japan

ARTICLE INFO

Keywords:
Fukushima Dai-ichi Nuclear Power Plant
Radioactive cesium
Marine sediment
Terrain features
Towed gamma ray spectrometer

ABSTRACT

An estimated $3.5 \pm 0.7 \times 10^{15}$ Bq of ^{137}Cs is thought to have been discharged into the ocean following the melt down at Fukushima Dai-ichi Nuclear Power Plant (F1NPP). While efforts have been made to monitor seafloor radiation levels, the sampling techniques used cannot capture the continuous distribution of radionuclides. In this work, we apply in situ measurement techniques using a towed gamma ray spectrometer to map the continuous distribution of ^{137}Cs on the seafloor within 20 km of the F1NPP. The results reveal the existence of local ^{137}Cs anomalies, with levels of ^{137}Cs an order of magnitude higher than the surrounding seafloors. The sizes of the anomalies mapped in this work range from a few meters to a few hundreds of meters in length, and it is demonstrated that the distribution of these anomalies is strongly influenced by meter scale features of the terrain.

1. Introduction

The melt down at Fukushima Dai-ichi Nuclear Power Plant (F1NPP) resulted in radioactive material being released into the environment, with an estimated $3.5 \pm 0.7 \times 10^{15}$ Bq of ^{137}Cs thought to have been discharged into the ocean between March 26 and the end of May 2011 (Tsumune et al., 2012). Whilst on land, survey efforts have revealed the distribution of ^{137}Cs in the environment (Yasunari et al., 2011; MEXT, 2013a), its distribution on the seafloor remains less clear due to the practical difficulties involved in surveying at sea. To date, monitoring of seafloor radiation levels has been performed through sampling (MEXT, 2013b,c). While the levels of ^{137}Cs in the affected region prior to the accident ranged from 0.68 to 1.7 Bq/kg (dry weight) (MEXT, 2011), values of several hundred Bq/kg are now common. The total inventory of ^{137}Cs accumulated in the upper 3 cm of surface sediments off the Miyagi, Fukushima and Ibaraki prefectures has been estimated to be 3.78×10^{13} Bq (Kusakabe et al., 2013), which is 0.9–1.4% of the total ^{137}Cs flux from the plant to the ocean estimated by Tsumune et al. (2012).

The distribution of ^{137}Cs on the seafloor determined from samples obtained off Fukushima shows considerable spatial variability in concentration, exhibiting no obvious correlation with proximity to the F1NPP. While remobilization of surface layers and local heterogeneity in the physical and chemical characteristics of the sediments have been identified as potential causes for the variability seen (Otosaka and Kobayashi, 2013), it has been pointed out that sediment mineralogy alone cannot completely account for the spatial distribution of ^{137}Cs in the sediments (Kusakabe et al., 2013). Furthermore, since the information obtained through sampling is discrete, with points often separated by several tens of kilometers, it is possible that variations in concentration exist on spatial scales that have not been captured through sampling. While this is not a problem in areas where it has been demonstrated that the levels of seafloor radiation change gradually (Thornton et al., 2013), the local scale distribution of radioactive material on the seafloor following the accident is largely unknown. The lack of information raises concerns regarding our ability to predict the effects of the accident on the marine ecosystem and limits our ability to form effective recovery strategies.

In this work, we apply in situ measurement techniques to map the continuous distribution of ^{137}Cs on the seafloor, and reveal the existence of a number of local ^{137}Cs anomalies within 20 km of F1NPP. The size and distribution of these anomalies is closely

* Corresponding author. Tel.: +81 30 5452 6489.
E-mail address: blair@iis.u-tokyo.ac.jp (B. Thornton).
[1] Address: Center for Socio-Robotic Synthesis, Kyushu Institute of Technology, 2–4, Hibikino, Wakamatsu, Kita-Kyushu 808–0196, Japan.

0025-326X
http://dx.doi.org/10.1016/j.marpolbul.2013.06.031

related to meter scale features of the seafloor terrain, and the concentrations of ^{137}Cs are often more than an order of magnitude higher than in the surrounding regions. The existence of these anomalies should be taken into account when planning future survey efforts, and when considering the potential effects of ^{137}Cs on marine ecology.

2. Instruments and methods

The instrument used in this work consists of a gamma ray spectrometer contained within a flexible rubber hose that is towed along the seafloor by a ship, as illustrated in Fig. 1 (Jones, 2001). The instrument, called the RESQ hose (RESQ: Radiometric Environment Survey and Quantification), is 8 m long with an external diameter of 0.145 m and weighs 135 kg in air and 115 kg in water. The compact size of the system allows it to be deployed from small fishing vessels and other ships of opportunity, which is particularly important for measurements in shallow waters near the shore that cannot be accessed using large research vessels. During operation, the system is attached to a wire that is used to lower it to the seafloor. Fig. 2 shows the device being lowered into the sea during a survey off Fukushima. The system has an internal battery that allows for up to 24 h continuous operation, and a data logging device that records the measurements of a depth sensor and a NaI(Tl) gamma ray scintillation spectrometer. The spectrometer has been calibrated to measure the gamma ray spectrum between 0.1 and 1.8 MeV over 1024 channels, and has a resolution of 6.9% at 0.662 MeV. The devices are covered using a rubber hose designed to reduce the risk of snagging, and provide protection from abrasion and impact damage during towing and handling on board the ship's deck, while maintaining enough flexibility for the system to follow the undulations of the seafloor. The system is towed at velocities of between 2 and 3 knots and can be operated at depths of up to 500 m.

The device was deployed during 4 cruises between November 2012 and February 2013 to measure over 140 km of continuous radionuclide distribution along 10 transects within a 20 km radius of F1NPP, shortly after the lifting of government restrictions on access to the area on August 10 2012 (MEXT, 2012). Over 113,000 seafloor gamma spectra were measured at a sampling rate of 1 Hz. The data has been quantified, geo-referenced and smoothed using the methods described by the authors in Thornton et al. (2013). The levels of ^{137}Cs have been determined through simulation using a Monte Carlo radiation transport model that computes the average concentration of the top 3 cm of the surface sediments, in accordance with sampling surveys (Kusakabe et al., 2013), based on the range of sediment types given in Table 1.

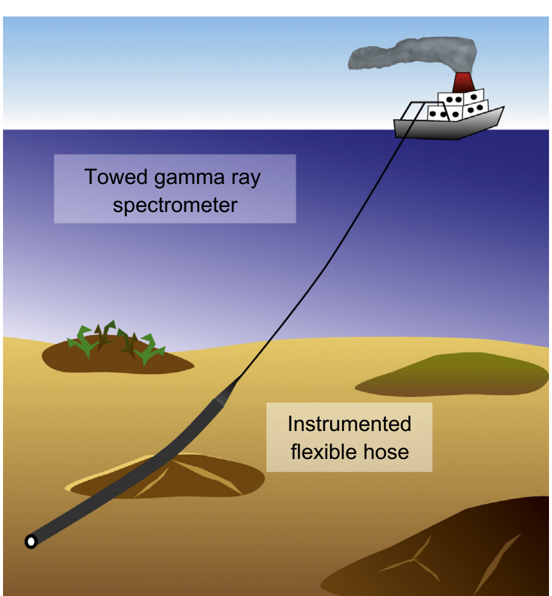

Fig. 1. Illustration of a ship towed gamma ray spectrometer (adapted from Jones (2001)).

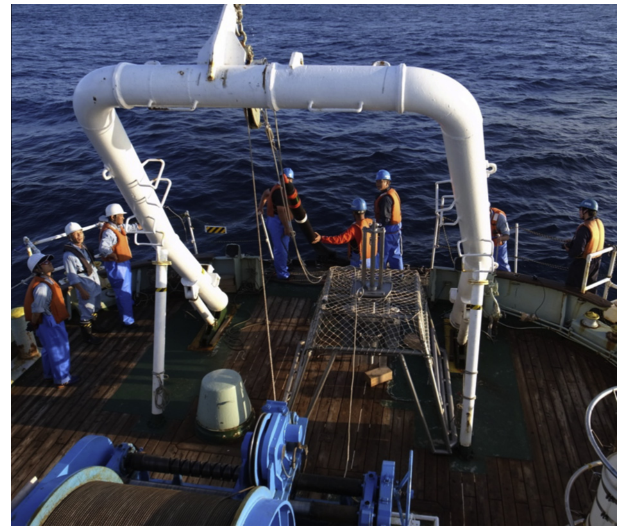

Fig. 2. Deployment of the towed gamma ray spectrometer off Fukushima.

Table 1
Sediment models used in the analysis. Values have been adapted from Hamilton (1971), Kato (1956), and Trask (1939).

Sediment type	ρ_{bulk} (g/cm^3)	Water content (% by mass)
Coarse sand	2.03	19.5
Fine sand	1.98	22.7
Very fine sand	1.91	25.4
Silty sand	1.83	29.6
Sandy silt	1.56	44.8
Sandy-silt–clay	1.58	43.7
Clayey silt	1.43	53.8
Silty clay	1.42	54.9
Inorganic (% by mass)	SiO_2 59.86, Al_2O_3 12.99, Fe_2O_3 4.42, CaO 2.14, MnO 1.03, P_2O_5 0.13	
Organic (% by mass)	C 5.28, N 0.57, H 0.75, O 3.01	

3. Results

Fig. 3 shows the continuous distribution of ^{137}Cs measured in Bq/kg (wet weight), where the colors indicate the mean values for the range of sediments modeled. The spatial resolution of the map has been optimized to satisfy a 1σ statistical measurement uncertainty of 5% of the measured value at each point. This is achieved using an inverse distance weighted window function with a 100 m limit imposed on the minimum resolution of the map, beyond which measurement uncertainty is allowed to increase. In areas with high levels of ^{137}Cs, the resolution of the map increases accordingly, where average ^{137}Cs levels of 250, 500, and 1000 Bq/kg would lead to resolutions of about 76, 38, and 19 m, respectively, with some variation depending on the local distribution of ^{137}Cs. The measurements show that the levels of ^{137}Cs are relatively high within 4 km of the coastline, averaging 292 Bq/kg (σ_v = 351 Bq/kg), where σ_v is the standard deviation of the measurements made in the area. Over 65% of the measurements in this region yield >200 Bq/kg, where the levels south of

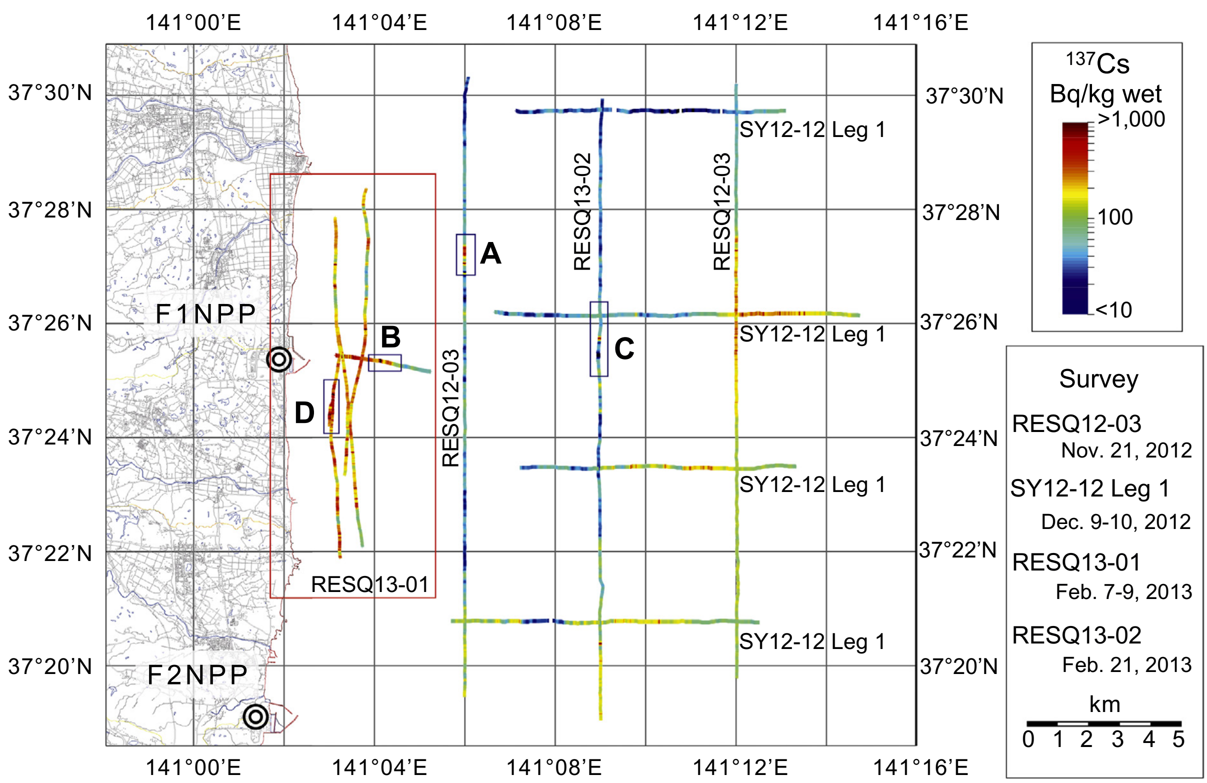

Fig. 3. ^{137}Cs levels on the seafloor within 20 km of the F1NPP. Measurements totaling over 140 km in length were made using a towed gamma ray spectrometer that was deployed during 4 cruises (6 days of measurement) between November 2012 and February 2013. The levels are determined for the top 3 cm of the surface sediments, where the average of the values calculated for the sediment types shown in Table 1 are taken, and are indicated by the color bar in the top right of the figure. Several of the ^{137}Cs anomalies (shown in Fig. 4) exceed the upper range of the color bar. The regions labeled A–D correspond to the profile plots in Fig. 5.

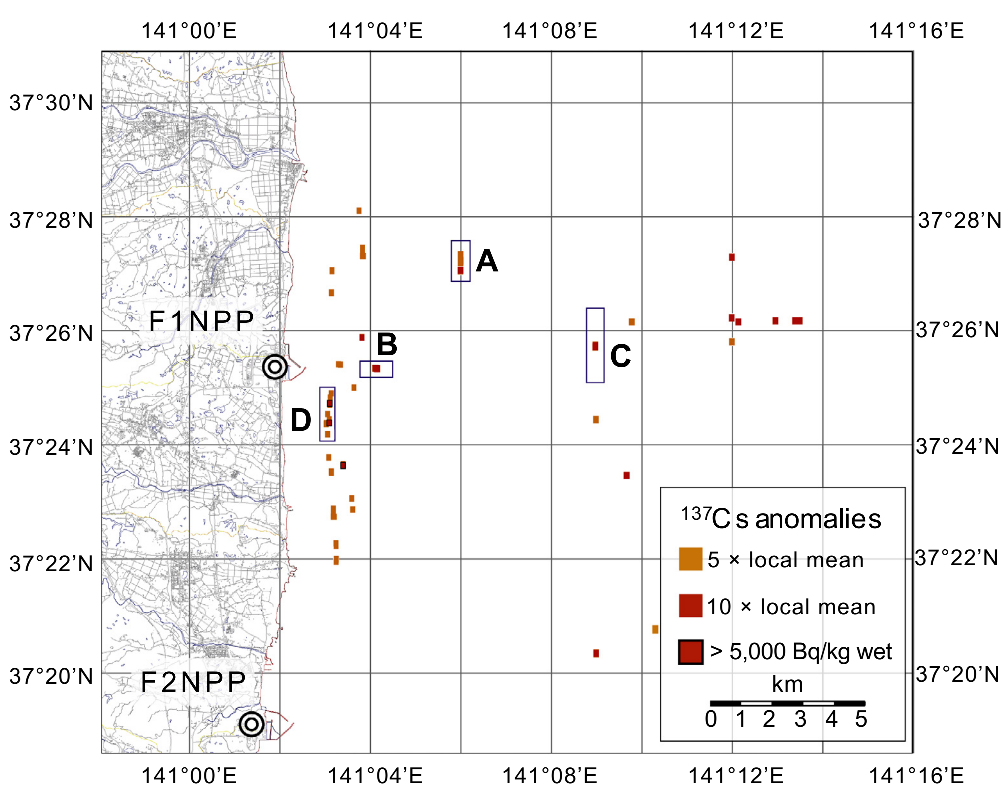

Fig. 4. Distribution of local ^{137}Cs anomalies on the seafloor. The locations where the levels of ^{137}Cs are a factor of 5 and a factor of 10 higher than the average of measurements made within a 2 km radius of each point are shown in orange and red, respectively. The regions highlighted with a black border correspond to anomalies where the maximum levels of ^{137}Cs measured are >5000 Bq/kg. The anomalies along the measured transects vary from a few meters to several hundreds of meters in length, and their distribution is strongly influenced by features of the underwater terrain.

the plant average 326 Bq/kg (σ_v = 441 Bq/kg), which is slightly higher and more variable than the levels north of the plant, which average 249 Bq/kg (σ_v = 168 Bq/kg). The highest levels of ^{137}Cs were recorded 1–2 km south of the plant with an average of 438 Bq/kg (σ_v = 867 Bq/kg). The large values of the standard deviations illustrate the strong variations in the levels of ^{137}Cs observed. The ^{137}Cs levels decrease further out from shore averaging 69 Bq/kg (σ_v = 73 Bq/kg) between 4 and 12 km from the coastline, with less than 3% of the measurements yielding >200 Bq/kg. The highest levels of contamination this distance from the shore average 128 Bq/kg (σ_v = 73 Bq/kg) between 8 and 10 km south of the plant. Beyond 12 km, the levels of ^{137}Cs increase to average 144 Bq/kg (σ_v = 163 Bq/kg), with over 20% of the measurements yielding >200 Bq/kg. The highest ^{137}Cs levels at this distance are between 0 and 4 km north of F1NPP, averaging 218 Bq/kg (σ_v = 270 Bq/kg). The observation that the concentrations of ^{137}Cs near the shore are higher south of the plant is consistent with sampling surveys and may be related to the high concentration of ^{137}Cs in seawater that flowed south from the plant following the accident (Kawamura et al., 2011; Masumoto et al., 2012; Miyazawa et al., 2012). The distribution further out to sea is also consistent with the results of sampling surveys, and is thought to be a function of the types of marine sediment found on the seafloor. The area up to 12 km from the shore is dominated by rocky outcrops (Fukushima Prefecture, 1996; Aoyagi and Igarashi, 1999), and the areas further out consist mainly of fine silty clays, which cesium has a high affinity for (Lieser et al., 1986; Lieser and Steinkopff, 1988; Cremers et al., 1988; Cornell, 1993; Boretzen and Salbu, 2002; IAEA, 2004).

While the measurements are consistent with the findings of sampling surveys, they also reveal the existence of a number of local anomalies in the levels of ^{137}Cs, which to date have not been captured by sampling. Fig. 4 shows the locations where the levels of ^{137}Cs are a factor of 5, and a factor of 10 higher than the average values of measurements made within a 2 km radius of each point. Although these anomalies account for only 0.9% of the measurements made, 30% of these measurements have ^{137}Cs levels >1000 Bq/kg, and all measurements >1000 Bq/kg in this work were made in these anomalies. The size of the anomalies varies from a few meters to several 100 m in length, and their distribution is strongly influenced by local features of the terrain. Anomalies have been consistently found at the bases of vertical features of the terrain, as seen in the examples in Fig. 5, which show the levels of ^{137}Cs measured together with the depth of the seafloor (the vertical axis of the depth profiles has been exaggerated for clarity of presentation). The margins represent the range of possible levels of ^{137}Cs taking into account the effects of different types of sediment

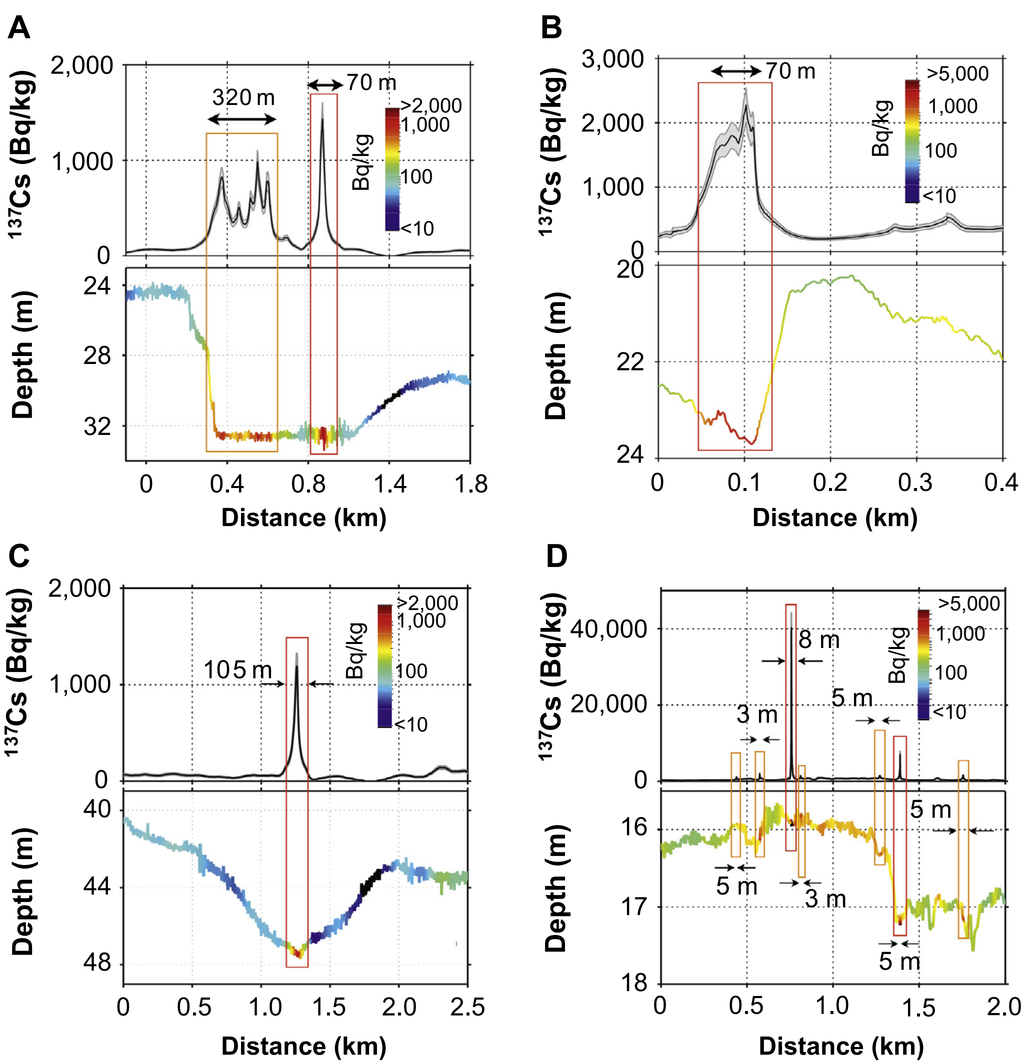

Fig. 5. Profiles of ^{137}Cs measurements made in the regions labeled A–D in Figs. 3 and 4. The shaded regions in the top graphs represent the range of uncertainty in the ^{137}Cs levels, taking into account the combined effects of different types of seafloor sediments on detector response and the statistical uncertainty in the measurements of the detector itself. The dark lines show the mean values, which are plotted in the color maps that show the depth profiles where the measurements were made. The vertical axis of the depth profiles has been exaggerated for clarity of presentation. A strong influence of terrain features on the distribution of ^{137}Cs is observed.

on the measurements of the detector, determined through Monte Carlo simulations, and the standard deviation in the measurements of the detector itself, as described in our previous work (Thornton et al., 2013). The upper bounds represent the levels determined for silty clays, and the lower bounds represent the levels determined for coarse sands, where all other sediment types modeled lie between these two boundaries. The dark lines represent the mean values for the range of sediments modeled, and correspond to the values shown in Fig. 3. The areas of seafloor shown in Fig. 5A and B both have high levels of ^{137}Cs recorded at the bases of vertical terrain features. The region in Fig. 5A, labeled A in Figs. 3 and 4, is an 8 m high southward facing feature of the terrain located 5.9 km from shore and 3.7 km north of F1NPP. While the levels of ^{137}Cs on top of the feature average 65 ± 9 Bq/kg (where the range of values represents measurement uncertainty), the average level of ^{137}Cs measured at its base within 320 m of the feature is 524 ± 63 Bq/kg, with a maximum value of 985 ± 118 Bq/kg in this patch. Another anomaly was mapped a few 100 m further on from the feature. The patch is 70 m in length, and averages 651 ± 77 Bq/kg with a maximum ^{137}Cs level of 1,432 ± 173 Bq/kg. The results show that the terrain strongly influences the level of ^{137}Cs, with more than an order of magnitude difference in the levels measured on top and at the base of the feature. Similar observations were made for the seafloor shown in Fig. 5B, which is a 3.5 m high feature located 3.2 km east of F1NPP. This region serves as a boundary for the radiation levels, with the seafloor on the plant side of the feature, 1.7–3.2 km from the plant along this transect averaging 446 ± 62 Bq/kg, and the levels on the other side of the feature, 3.4–4.9 km from the plant yielding an average of 133 ± 17 Bq/kg. The level of ^{137}Cs at the base of the feature has a maximum value of 2276 ± 266 Bq/kg, with an average of 1534 ± 175 Bq/kg over the 70 m long patch. The seafloor in Fig. 5C shows an anomaly in a depression located 10.3 km east and 0.7 km north of the F1NPP. The highest level of ^{137}Cs in this patch is 1190 ± 136 Bq/kg, with an average of 508 ± 58 Bq/kg over the 105 m length of the anomaly measured along the transect. Here the size of the depression bounds the dimensions of the anomaly, and it is clear that features of the terrain influence not only the distribution, but also the size of the anomalies identified in this work.

In addition to terrain related anomalies, anomalies have also been identified in areas with no noticeable features of the seafloor. The seafloor shown in Fig. 5D, located 1.6 km east of the F1NPP between 0.2 km and 2.2 km south of the plant, has particularly high levels of ^{137}Cs averaging 528 ± 67 Bq/kg. The highest level of ^{137}Cs recorded in this region is 40,152 ± 3998 Bq/kg, with two other locations nearby where the levels of ^{137}Cs measured are >5000 Bq/kg. These anomalies are extremely local with only a few meters of the seafloor affected along the measured transects. While measurements >5000 Bq/kg account for only 0.0012% of the measurements made in this work, the possibility of high concentration particulate matter being present in these areas must be considered. It is clear that extensive sampling of the identified regions is necessary to determine the cause of these anomalies.

4. Discussion

While it has been demonstrated that the well documented affinity of ^{137}Cs to fine-grained sediments determines the overall distribution of ^{137}Cs on the seafloor (Otosaka and Kobayashi, 2013), it has also been pointed out that sediment mineralogy alone cannot completely account for the spatial distributions observed along the east coast of Japan (Kusakabe et al., 2013). With regard to this point, the influence of the original distribution of ^{137}Cs in the water column has been identified as a potential cause by Oikawa et al., (2013), who describe a scenario for rapid downward migration of ^{137}Cs in the water column. While the majority of ^{137}Cs in the water column is known to be in the form of dissolved ions (Stanners and Aston, 1981; Nies et al., 1991; Knapinska-Skiba

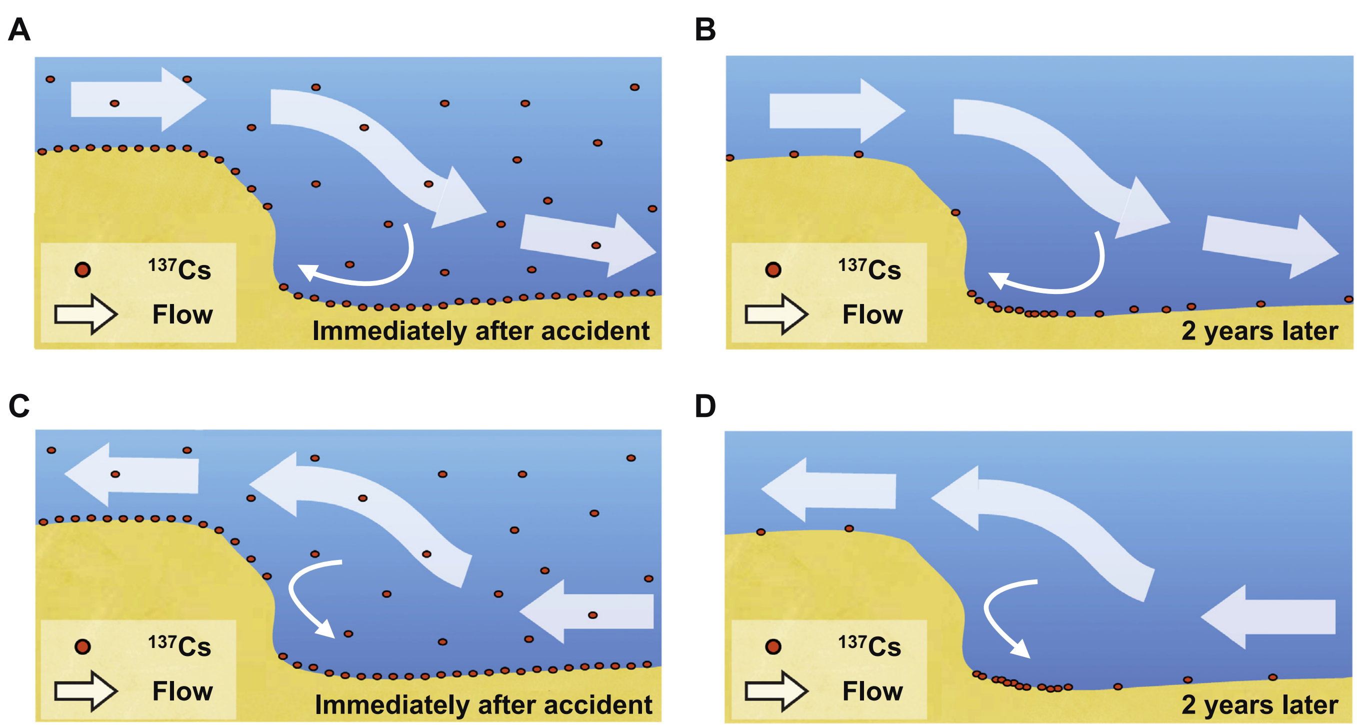

Fig. 6. A conceptual model of the mechanisms thought to be responsible for the terrain related anomalies identified in this work. (A and C) The illustrations represent a snapshot of the situation immediately after the input of ^{137}Cs, showing locally homogenous (on the scale of a few 100 m) distribution of ^{137}Cs bound to particles in the water column, which sink to the seafloor due to gravity processes. (B and D) The illustrations show the same area some years later, i.e. when measurements were made. Sediments with high concentrations of ^{137}Cs have been dispersed in areas exposed to underwater currents, whereas in areas shielded from underwater currents by features of the terrain the high concentration sediments remain locally confined. The depth profile in the illustration has been exaggerated for clarity of presentation.

et al., 1994; Lujaniene et al., 2004, 2010), it has been shown that once ^{137}Cs is incorporated into particulate matter, it is rapidly removed from seawater to the bottom sediment with reported settling velocities ranging from 29 to 190 m day^{-1} (Fowler et al., 1987; Kusakabe et al., 1988). The unusual sedimentary environment resulting from suspended load carried back from land by the tsunami may also have contributed to rapid removal of nuclides from seawater (Kusakabe et al., 2013).

Fig. 6 shows a conceptual model for the mechanisms thought to be responsible for the observed relation between features of the terrain and the high level ^{137}Cs anomalies recorded in this work. Fig. 6A and C show two snapshots of the situation shortly after contamination, where the underwater currents flow in opposite directions normal to a vertical feature of the terrain. Field observations of currents at a depth of 20 m, 30 km off F1NPP by Miyazawa et al. (2012) indicate that the mean currents in the region are relatively weak with velocities typically less than 0.4 m/s. Diurnal cycling of the currents along the north–south direction occurs due to wind effects, and simulations performed in their study demonstrate that tidal currents and river discharge flows also have a moderate impact on the transport of dissolved ^{137}Cs. Since rapidly sinking particles are thought to be responsible for transport of ^{137}Cs from the water column to the sediments (Fowler et al., 1987; Kusakabe et al., 1988; Oikawa et al., 2013; Kusakabe et al., 2013), it is reasonable to assume that the horizontal distribution of sinking ^{137}Cs particles in the water column would be relatively homogeneous over the scale of a few 100 m at any moment in time. Since the downward flux of sinking particulate matter is largely dependent on the dimensions of the particles and gravity processes (Gardner and Walsh, 1990; Klaas and Archer, 2002; Buesseler et al., 2007), it follows that the distribution of contaminated particles reaching the seafloor at any moment would also be relatively homogenous. Fig. 6B and D show the corresponding situation 2 years later, roughly when the observations were made. In the illustrations, the contaminated particulate matter in the water column has subsided, and contaminated sediments in areas exposed to underwater currents have been remobilized and dispersed (Otosaka and Kobayashi, 2013). In areas where the seafloor is shielded from currents by the terrain, even though particle re-suspension would allow for some vertical and horizontal mixing (Gardner et al., 1985), the range of horizontal motion would be limited, with a tendency for pockets of contaminated fine-grained sediments to remain confined due to the energy lowering effects of the terrain and its influence on the local patterns of flow (Kennish, 2001). While it is necessary to verify the model through analysis of sediments sampled in the affected areas, the implications of the model are that the levels of ^{137}Cs in these anomalies are likely to remain relatively unchanged over the timescales of a few years due to the effects of the local terrain on sediment transport. The influence of such features of the terrain should be considered together with other factors that can influence the distribution of ^{137}Cs in the marine environment, such as secondary contamination from ground water and river inlets (Yoshida and Kanda, 2012; Nagao et al., 2013).

5. Conclusions

The measurements made in this work have revealed the existence of several ^{137}Cs anomalies on the seafloor within 20 km of F1NPP. A strong correlation between the size and distribution of anomalies and features of the terrain has been demonstrated, with anomalies consistently found at the bases of vertical features of the terrain where the pockets of sediments are sheltered from underwater currents. It is clear from the results of this study that fine, meter scale features of the seafloor terrain play a significant role in determining the distribution of ^{137}Cs on the seafloor within 20 km of the F1NPP.

Based on the size and distribution of the anomalies mapped in this work, it can be said that the density of sampling points required to survey this region effectively using a standard grid based approach would be impractical and the costs associated with such an effort would be prohibitive. It is clear that a more targeted approach to sampling based on prior screening using in situ measurement techniques is necessary. The approach described in this work should be combined with wide area acoustic surveys to determine the distribution of fine-grained sediments off F1NPP. Direct observations of the nature of the seafloor in the areas identified are necessary together with targeted sampling efforts in order to achieve a better understanding of the processes involved for the different types of anomaly identified in this work, i.e. (1) 100 m scale terrain related anomalies, and (2) more localized meter scale anomalies showing no correlation with features of the terrain. It is hoped that the results described can help focus future survey and recovery efforts, and so advance our understanding of the potential effects of the accident on the marine environment.

Acknowledgments

The authors thank the Radioisotope Center of the University of Tokyo, the Marine Ecology Research Institute of Japan, Nippon-kaiyo, and Hakuyodo, in particular Naoki Kosaka, Jun Misonoo, Masashi Kusakabe, Hideo Oda, Tomohide Yamamoto, Daisuke Andou, Yusuke Yano and the crew of the R/V Kaiyomaru No. 7, the R/V Kotakamaru, the R/V Soyomaru, and Shizumaru for their support leading up to and during the deployments of the towed gamma ray spectrometer. This research is funded by the Fisheries Agency of Japan's fund for emergency investigation of mechanisms for radioactive contamination of marine life, and the Mitsui & Co., Ltd. Support Fund for Environmental Survey.

References

Aoyagi, K., Igarashi, S., 1999. On the size and distribution of sediments in the coastal sea of Fukushima prefecture. Bull. Fukushima Prefect. Fish. Exp. Station 8, 69–81 (in Japanese).

Boretzen, P., Salbu, B., 2002. Fixation of Cs to marine sediments estimated by a stochastic modeling approach. J. Environ. Radioact. 61, 1–20.

Buesseler, K.O. et al., 2007. An assessment of the use of sediment traps for estimating upper ocean particle fluxes. J. Mar. Res. 65, 345–416.

Cornell, R.M., 1993. Adsorption of cesium on minerals: a review. J. Radioanal. Nucl. Chem. 171, 483–500.

Cremers, A., Elsen, A., De Preter, P., Maes, A., 1988. Quantitative analysis of radiocaesium retention in soils. Nature 335, 247–249.

Fowler, S.W., Buat-Menard, P., Yokoyama, Y., Ballestra, S., Holm, E., Nguyen, H.V., 1987. Rapid removal of chernobyl fallout from mediterranean surface water by biological activity. Nature 329, 56–58.

Fukushima Prefecture, Department of Agriculture, Forestry and Fisheries, Fisheries Division, 1996. Fukushima Prefecture Coastal Map. Report of the 1995 Program for the Promotion Regional Activity and Structural Reform, pp. 1–18 (in Japanese).

Gardner, W.D., Southard, J.B., Hollister, C.D., 1985. Sedimentation, resuspension and chemistry of particles in the Northwest Atlantic. Mar. Geol. 65, 199–242.

Gardner, W.D., Walsh, I.D., 1990. Distribution of macroaggregates and fine-grained particles across a continental margin and their potential role in fluxes. Deep Sea Res. 35, 401–411.

Hamilton, E.L., 1971. Elastic properties of marine sediments. J. Geophys. Res. 76, 579–604.

IAEA, 2004. Sediment distribution coefficients and concentration factors for Biota in the Marine Environment. IAEA Tech. Report Series 422, 1–95.

Jones, D.G., 2001. Development and application of marine gamma ray measurements: a review. J. Environ. Radioactiv. 53, 313–333.

Kato, K., 1956. Chemical investigations on marine humus in bottom sediments. Mem. Faculty Fish Hokkaido Univ. 4, 91–209.

Kawamura, H. et al., 2011. Preliminary numerical experiments on oceanic dispersion of ^{131}I and ^{137}Cs discharged into the ocean because of the Fukushima Daiichi Nuclear Power Plant Disaster. J. Nucl. Sci. Technol. 48, 1349–1356.

Kennish, M.J., 2001. Practical Handbook of Marine Science, third ed.. CRC Press, Boca Raton, Florida, 1–876.
Klaas, C., Archer, D.E., 2002. Association of sinking organic matter with various types of mineral ballast in the deep sea: implications for the rain ratio. Global Biogeochem. Cycles 16, 1–14.
Knapinska-Skiba, D., Bojanowski, R., Radecki, Z., 1994. Sorption and release of radiocaesium from particulate matter of the Baltic coastal zone, Netherland. J. Aquat. Ecol. 28, 413–419.
Kusakabe, M., Ku, T.L., Harada, K., Taguchi, K., Tsunogai, S., 1988. Chernobyle radioactivity found in mid-water sediment trap interceptor in the N. Pacific and Bering Sea. Geophys. Res. Lett. 15, 44–47.
Kusakabe, M., Oikawa, S., Takata, H., Misonoo, J., 2013. Spatiotemporal distributions of Fukushima-derived radionuclides in surface sediments in the waters off Miyagi, Fukushima, and Ibaraki Prefectures, Japan. Biogeosci. Discuss. 10, 4819–4850.
Lieser, K.H., Gleitsmann, B., Steinkopff, T., 1986. Sorption of trace-elements or radionuclides in natural systems containing groundwater and sediments. Radiochim. Acta 40, 33–37.
Lieser, K.H., Steinkopff, T., 1988. Chemistry of radioactive cesium in the hydrosphere and in the geosphere. Radiochim. Acta 46, 39–47.
Lujaniene, G., Silobritiene, B., Joksas, K., Morkuniene, R., 2004. Behaviour of radiocesium in the marine environment. Environ. Res., Eng. Manage. 2, 23–32.
Lujaniene, G. et al., 2010. Experimental study and modelling of ^{137}Cs sorption behavior in the Baltic Sea and the Curonian Lagoon. J. Radioanal. Nucl. Chem. 286, 361–366.
Masumoto, Y. et al., 2012. Oceanic dispersion simulations of ^{137}Cs released from the Fukushima Daiichi Nuclear Power Plant. Elements 8, 207–212.
MEXT: Ministry of Education, Culture, Sports, Science and Technology-Japan, Monitoring information of environmental radioactivity level, Seafloor monitoring report, 2011. <http://www.radioactivity.nsr.go.jp/ja/contents/4000/3857/24/1305744_0527.pdf> (published online May 2011).
MEXT: Ministry of Education, Culture, Sports, Science and Technology-Japan, Restricted areas and areas to which evacuation orders have been issued, 2012. <http://www.meti.go.jp/english/earthquake/nuclear/roadmap/pdf/20121130_01.pdf> (published online November, 2012).
MEXT: Ministry of Education, Culture, Sports, Science and Technology-Japan. (i) Results of the sixth airborne monitoring and (ii) Airborne monitoring out of the 80km zone of Fukushima Dai-ichi NPP, 2013a. <http://www.radioactivity.nsr.go.jp/en/contents/7000/6099/24/203_e_0301_18.pdf> (published online March, 2013).
MEXT: Ministry of Education, Culture, Sports, Science and Technology-Japan. Readings of sea area monitoring at offshore of Miyagi, Fukushima, Ibaraki and Chiba Prefecture (Including Sr) (marine soil), 2013b. <http://www.radioactivity.nsr.go.jp/en/contents/7000/6090/24/229_so_mfic_Sr_0322_14.pdf> (published online March, 2013).
MEXT: Ministry of Education, Culture, Sports, Science and Technology-Japan. Distribution map of radioactivity concentration in the marine soil around coast of Fukushima prefecture and Fukushima Dai-ichi NPP (Converted as dry soil), 2013c. <http://www.radioactivity.nsr.go.jp/en/contents/7000/6177/24/20130322-02.pdf> (published online March, 2013).
Miyazawa, Y., Masumoto, Y., Varlamov, S.M., Miyama, T., 2012. Transport simulation of the radionuclide from the shelf to open ocean around Fukushima. Cont. Shelf Res. 50, 16–29.
Nagao, S. et al., 2013. Export of ^{134}Cs and ^{137}Cs in the Fukushima river systems at heavy rains by typhoon Roke in September 2011. Biogeosci. Discuss. 10, 2767–2790.
Nies, H., Albrecht, H., Herrmann, J., 1991. Radionuclides in water and suspended particulate matter from the North Sea. In: Kershaw, P.J., Woodhead, D.S. (Eds.), Radionuclides in the Study of Marine Processes. Springer, Netherlands, pp. 24–36.
Oikawa, S., Takata, H., Watabe, T., Misonoo, J., Kusakabe, M., 2013. Distribution of the Fukushima-derived radionuclides in seawater in the Pacific off the coast of Miyagi, Fukushima, and Ibaraki Prectures, Japan. Biogeosci. Discuss. 10, 4851–4886.
Otosaka, S., Kobayashi, T., 2013. Sedimentation and remobilization of radiocesium in the coastal area of Ibaraki, 70 km south of the Fukushima Dai-ichi Nuclear Power Plant. Environ. Monit. Assess. 185, 5419–5433.
Stanners, D.A., Aston, S.R., 1981. Factors Controlling the Interactions of ^{137}Cs with Suspended and Deposited Sediments in Estuarine and Coastal Environments, In Impacts of Radionuclide Releases into the Marine Environment. International Atomic Energy Agency, Vienna, 131–141.
Thornton, B., Ohnishi, S., Ura, T., Odano, N., Fujita, T., 2013. Continuous measurement of radionuclide distribution off Fukushima using a towed sea-bed gamma ray spectrometer. Deep-sea Res. pt. 1 (79), 10–19.
Trask, P.D., 1939. Organic content of recent marine sediments. In: Trask, P.D. (Ed.), Recent Marine Sediments. Dover Publications, New York, pp. 428–453.
Tsumune, D., Tsubono, T., Aoyama, M., Hirose, K., 2012. Distribution of oceanic ^{137}Cs from the Fukushima Dai-ichi Nuclear Power Plant simulated numerically by a regional ocean model. J. Environ. Radioactive 111, 100–108.
Yasunari, J.T. et al., 2011. Cesium-137 deposition and contamination of Japanese soils due to the Fukushima nuclear accident. PNAS. http://dx.doi.org/10.1073/pnas.1112058108.
Yoshida, N., Kanda, K., 2012. Tracking the Fukushima radionuclides. Science 336, 1115–1116.